Navigation Systems Based on Multiple Bearing Measurements

Pedro Batista, Carlos Silvestre, and Paulo Oliveira

IEEE Transactions on Aerospace and Electronic Systems, vol. 51, no. 4, pp. 2887-2899, October 2015

https://doi.org/10.1109/TAES.2015.140515

Navigation Systems based on Multiple Bearing Measurements

Pedro Batista, *Member, IEEE*, Carlos Silvestre, *Member, IEEE*, and Paulo Oliveira, *Senior Member, IEEE*

***Abstract*—This paper presents two navigation filters based on multiple bearing measurements. In the first, the state is augmented and an equivalent linear system is derived, while in the second the output of the system is modified in such a way that the resulting system is linear. In both cases, the design of a filtering solution relies on linear systems theory, in spite of the nonlinear nature of the system, and the resulting error dynamics can be made globally exponentially stable applying, e.g., Kalman filters. The continuous-discrete nature of the different measurement sources is taken into account, with the updates occurring in discrete-time, while open-loop propagation is carried out between bearing measurements. Simulation results are presented, including Monte Carlo runs and a comparison with both the extended Kalman filter and the Bayesian Cramér-Rao bound, to assess the performance of the proposed solutions.**

***Index Terms*—Navigation; bearings; long baseline.**

I. Introduction

A common problem in the development of autonomous vehicles, as well as sophisticated human-operated vehicles, is that of designing the navigation system. While many different solutions exist, (pseudo-)distance measurements, particularly to more than one landmark, is one of the most popular choices, very effective in long baseline (LBL) configurations. This paper considers bearing measurements to multiple landmarks as an alternative to distance measurements in the design of navigation systems, and two different solutions are proposed.

The celebrated global positioning system (GPS) is usually the workhorse of the navigation systems designed for open-space operation, see e.g. [1] and references therein. In underwater applications LBL acoustic positioning systems are often employed, as the electromagnetic waves suffer from significant attenuation in this medium, preventing the use of GPS. In [2] three acoustic transponders, with known inertial positions, are considered and an extended Kalman filter (EKF), coupled with a smoothing algorithm, is proposed to estimate the system state. In [3] a typical LBL positioning system is combined with a Doppler sonar, as well as a magnetometer and roll/pitch sensors, and complementary filtering concepts are applied to show that the LBL rate and the Doppler precision can be improved. In [4] two different strategies are presented. In the so-called fix computation approach, dead-reckoning is performed between acoustic fixes, which reset the vehicle position whenever available. In the second approach, so-called filtering approach, dead-reckoning is performed but, whenever available, travel-times are used to correct drift resulting from dead-reckoning. Preliminary fields trials are reported in [5], where a navigation system that employs a LBL acoustic positioning system, a Doppler sonar, a fiber-optic North seeking gyro, pressure sensors and magnetic compasses is used. A different concept, where one aims to estimate a segment of the trajectory instead of the current position, is proposed in [6], where diffusion-based trajectory observers are considered.

The use of single range measurements as a cheaper alternative to LBL navigation has been considered in several recent contributions, leveraging also on results for target localization based on range measurements. In [7] a recursive least squares fading memory filtering solution is proposed for the later, and the dependence of the covariance of the estimated target on the velocity profile of the vehicle is discussed. An extended Kalman filter is proposed in [8] as a solution to the problem of navigation based on range measurements to a single source, while an algebraic approach to the same problem can be found in [9]. A complete integrated navigation system, aided by range measurements, is simulated [10], where a multirate extended Kalman filter provides the filtering solution. The duality between navigation and source localization based on single range measurements is evidenced in [11], where a novel solution is also proposed with globally exponentially stable error dynamics.

An alternative to single range measurements is the use of bearing measurements, see e.g. [12], where the estimation error dynamics were shown to be globally exponentially stable (GES) under an appropriate persistent excitation condition and a circumnavigation control law was also proposed. Earlier work on the observability issues of target motion analysis based on angle readings, in 2-D, can be found in [13], which was later extended to 3-D in [14]. The specific observability criteria thereby derived resort to complicated nonlinear differential equations and some tedious mathematics are needed for the solution, giving conditions that are necessary for system observability. The problem of localization of a mobile robot using bearing measurements was also addressed in [15], where a nonlinear transformation of the measurement equation into a higher dimensional space is performed. This has allowed to obtain tight, possibly complex-shaped, bounding sets for the feasible states in a closed-form representation. The problem of bearings-only target motion analysis was considered in [16], where its observability was discussed in a discrete-time setup and some insights to the optimization of observer maneuvers were provided. The posterior Cramér-Rao bounds were later

This work was partially supported by the FCT [UID/EEA/50009/2013]] and through IDMEC, under LAETA FCT [UID/EMS/50022/2013] projects, and by Macao Science & Technology Development Fund (FDCT) through Grant FDCT/065/2014/A and by project MYRG2015-00127-FST of the University of Macau.

The authors are with the Institute for Systems and Robotics, Laboratory for Robotics and Engineering Systems, Portugal. Pedro Batista is also with the Department of Electrical and Computer Engineering, Instituto Superior Técnico, Universidade de Lisboa, Portugal. Carlos Silvestre is also with the Department of Electrical and Computer Engineering, Faculty of Science and Technology, University of Macau, Taipa, Macau, China, on leave from Instituto Superior Técnico, Universidade de Lisboa, Portugal. Paulo Oliveira is also with the Department of Mechanical Engineering, Instituto Superior Técnico, Universidade de Lisboa, Portugal.

Emails: {pbatista,cjs,pjcro}@isr.ist.utl.pt

discussed in [17] and a hierarchical particle filter proposed in [18]. An alternative solution, based on the Cubature Kalman filter, was presented in [19].

In previous work by the authors [20] the problems of source localization and navigation based on bearing measurements to a single source were addressed in a continuous-time framework, where the duality between both problems is again evidenced. In practice, the bearing measurements are often acquired in discrete-time, which poses challenge both in terms of observability analysis and filter design, which led to the extension presented in [21], where discrete-time bearing measurements, to a single source, are considered.

This paper addresses the problem of navigation based on multiple bearing measurements. More specifically, the vehicle is assumed equipped with a relative velocity sensor, an attitude and heading reference system (AHRS), and bearing sensors, and aims to estimate its inertial position and velocity. To solve the problem, two different solutions are proposed: i) in the first solution, state augmentation is performed, including the range in the system state, and an artificial output is derived such that the system as a whole is linear in the state; and ii) in the second solution, the original nonlinear output is rewritten in such a way that the system is linear in the state, even though no state augmentation is performed. Common to both solutions is a constructive observability analysis, using linear systems theory, which enables the design of Kalman filters with globally exponentially stable error dynamics. The multirate characteristics of the sensors are also accounted for in both filter designs.

The paper is organized as follows. In Section II the problem considered in the paper and the nominal system dynamics are introduced. The first solution is derived and analyzed in Section III, whereas the second solution is presented in Section IV. Simulation results, including Monte Carlo runs and comparison with both the extended Kalman filter and the Bayesian Cramér-Rao Bound, are discussed in Section V. Finally, Section VI summarizes the main results of the paper.

A. Notation

Throughout the paper the symbols $\mathbf{0}$ and $\mathbf{I}$ denote a matrix of zeros and the identity matrix, respectively, while $\operatorname{diag}(\mathbf{A}_1, \ldots, \mathbf{A}_\mathrm{n})$ is a block diagonal matrix. The Special Orthogonal Group is denoted by $SO(3) := \left\{\mathbf{X} \in \mathbb{R}^{3\times 3} : \mathbf{X}^T\mathbf{X} = \mathbf{I}, \det(\mathbf{X}) = 1\right\}$ and the set of unit vectores is defined as $S(2) := \left\{\mathbf{x} \in \mathbb{R}^3 : \|\mathbf{x}\| = 1\right\}$.

II. Problem statement

Consider a vehicle moving in a mission scenario where a set of landmarks are fixed and suppose that the vehicle measures the bearing to each of the landmarks. The vehicle is assumed to be moving relatively to a fluid, which has constant velocity. Further consider that the vehicle is equipped with a relative velocity sensor and an AHRS that provides its attitude. The problem considered in this paper is that of designing an estimator for the position and velocity of the vehicle based on the available data.

Denote by $\{I\}$ an inertial coordinate reference frame and by $\{B\}$ a coordinate frame attached to the vehicle, usually called the body-fixed frame. Let $\mathbf{p}(t) \in \mathbb{R}^3$ be the inertial position of the vehicle and denote by $\mathbf{v}(t) \in \mathbb{R}^3$ its inertial velocity, expressed in $\{I\}$, such that $\dot{\mathbf{p}}(t) = \mathbf{v}(t)$. Let the inertial velocity of the fluid be $\mathbf{v}_f(t) \in \mathbb{R}^3$, expressed in inertial coordinates, and denote by $\mathbf{v}_r(t) \in \mathbb{R}^3$ the velocity of the vehicle relative to the fluid, expressed in $\{B\}$, as measured by the relative velocity sensor. As such,

$$\mathbf{v}(t) = \mathbf{R}(t)\mathbf{v}_r(t) + \mathbf{v}_f(t),$$

where $\mathbf{R}(t) \in SO(3)$ is the rotation matrix from $\{B\}$ to $\{I\}$, which is provided by the AHRS. Finally, let $\mathbf{s}_i \in \mathbb{R}^3$, $i = 1, \ldots, L$, denote the inertial positions of the landmarks. Then, the bearing measurements are given by

$$\mathbf{d}_i(k) = \mathbf{R}^T(t_k)\,\frac{\mathbf{s}_i - \mathbf{p}(t_k)}{\|\mathbf{s}_i - \mathbf{p}(t_k)\|} \in S(2), i = 1, \ldots, L, \quad (1)$$

with $t_k = t_0 + kT$, $k \in \mathbb{N}$, where $T > 0$ is the sampling period and t_0 is the initial time.

Assuming that the velocity of the fluid $v_f(t)$ is constant, the nominal system dynamics can be written as

$$\begin{cases} \dot{\mathbf{p}}(t) & = \mathbf{v}_f(t) + \mathbf{R}(t)\mathbf{v}_r(t) \\ \dot{\mathbf{v}}_f(t) & = \mathbf{0} \\ \mathbf{d}_1(k) & = \mathbf{R}^T(t_k)\,\frac{\mathbf{s}_1 - \mathbf{p}(t_k)}{\|\mathbf{s}_1 - \mathbf{p}(t_k)\|} \\ \vdots & \\ \mathbf{d}_L(k) & = \mathbf{R}^T(t_k)\,\frac{\mathbf{s}_L - \mathbf{p}(t_k)}{\|\mathbf{s}_L - \mathbf{p}(t_k)\|} \end{cases}. \quad (2)$$

The problem considered here is that of designing an estimator for the nonlinear continuous-discrete system (2), given $\mathbf{v}_r(t)$, $\mathbf{R}(t)$, and $\mathbf{d}_i(t_k)$, $i = 1, \ldots, L$, with globally exponentially stable error dynamics.

A. Discrete-time system dynamics

As the bearing measurements, which are used to drive the estimation error to zero, are only available at discrete-time instants, it is of interest to compute the equivalent discrete-time system dynamics, which are given by

$$\begin{cases} \mathbf{p}(t_{k+1}) = \mathbf{p}(t_k) + T\mathbf{v}_f(t_k) + \mathbf{u}(k) \\ \mathbf{v}_f(t_{k+1}) = \mathbf{v}_f(t_k) \\ \mathbf{d}_1(k) = \mathbf{R}^T(t_k)\,\frac{\mathbf{s}_1 - \mathbf{p}(t_k)}{\|\mathbf{s}_1 - \mathbf{p}(t_k)\|} \\ \vdots \\ \mathbf{d}_L(k) = \mathbf{R}^T(t_k)\,\frac{\mathbf{s}_L - \mathbf{p}(t_k)}{\|\mathbf{s}_L - \mathbf{p}(t_k)\|} \end{cases}, \quad (3)$$

with

$$\mathbf{u}(k) := \int_{t_k}^{t_{k+1}} \mathbf{R}(\tau)\,\mathbf{v}_r(\tau)\,d\tau.$$

In practice, one aims at determining an estimator for the discrete-time nonlinear system (3), as the measurements that are used to drive the estimation error to zero are available in discrete-time. As the other measurements are available in continuous-time (or at high rates), open-loop propagation of the state estimates can be carried out between bearing updates to yield estimates in continuous-time (or at high rates). This will be detailed later on.

III. Filter design with state augmentation

A. State augmentation

This section details a state augmentation procedure that allows to obtain a linear system useful for the design of an estimator for the nonlinear system (3). In short, the distances to each landmark are added to the system state, their dynamics are derived, as a function of the whole state, and the output is redefined considering the added states so that the system can be regarded as linear.

Define as system states

$$\begin{cases} \boldsymbol{x}_1(k) := \mathbf{p}(t_k) \\ \boldsymbol{x}_2(k) := \mathbf{v}_f(t_k) \\ x_3(k) := \|\mathbf{s}_1(k) - \mathbf{p}(t_k)\| \\ \vdots \\ x_{2+L}(k) := \|\mathbf{s}_L(k) - \mathbf{p}(t_k)\| \end{cases},$$

where the distances between each landmark and the vehicle are included as additional states. In order to derive the dynamics of the additional states, notice that it is possible to write, from (1), that

$$x_{2+i}(k+1)\,\mathbf{d}_i(k+1) = \mathbf{R}^T(t_{k+1})\left[\mathbf{s}_i - \boldsymbol{x}_1(k+1)\right], \quad (4)$$

$i = 1, \ldots, L$. Now, left multiplying both sides of (4) by $\mathbf{d}_i^T(k+1)$ and using the dynamics for $\boldsymbol{x}_1(k)$ given by (3) yields

$$\begin{aligned} x_{2+i}(k+1) = {} & \mathbf{d}_i^T(k+1)\,\mathbf{R}^T(t_{k+1})\,\mathbf{s}_i \\ & -\mathbf{d}_i^T(k+1)\,\mathbf{R}^T(t_{k+1})\,\boldsymbol{x}_1(k) \\ & -T\mathbf{d}_i^T(k+1)\,\mathbf{R}^T(t_{k+1})\,\boldsymbol{x}_2(k) \\ & -\mathbf{d}_i^T(k+1)\,\mathbf{R}^T(t_{k+1})\,\mathbf{u}(k),\, i = 1, \ldots, L. \end{aligned} \quad (5)$$

The evolution of $x_{2+i}(k)$ described by (5) is undesirable as $x_{2+i}(k+1)$ does not depend on $x_{2+i}(k)$. In order to avoid that, take (4) at time t_k, which gives

$$x_{2+i}(k)\,\mathbf{d}_i(k) = \mathbf{R}^T(t_k)\left[\mathbf{s}_i - \boldsymbol{x}_1(k)\right], i = 1, \ldots, L. \quad (6)$$

Left multiplying both sides of (6) by $\mathbf{R}(t_k)$ gives

$$\mathbf{s}_i - \boldsymbol{x}_1(k) = x_{2+i}(k)\mathbf{R}(t_k)\,\mathbf{d}_i(k),$$

which allows to rewrite (5) as

$$\begin{aligned} x_{2+i}(k+1) = {} & -T\mathbf{d}_i^T(k+1)\,\mathbf{R}^T(t_{k+1})\,\boldsymbol{x}_2(k) \\ & +\mathbf{d}_i^T(k+1)\,\mathbf{R}^T(t_{k+1})\,\mathbf{R}(t_k)\,\mathbf{d}_i(k)x_{2+i}(k) \\ & -\mathbf{d}_i^T(k+1)\,\mathbf{R}^T(t_{k+1})\,\mathbf{u}(k),\, i = 1, \ldots, L. \end{aligned} \quad (7)$$

Finally, left multiply both sides of (4) by $\mathbf{R}(t_{k+1})$, which allows to write

$$\boldsymbol{x}_1(k+1) + x_{2+i}(k+1)\,\mathbf{R}(t_{k+1})\,\mathbf{d}_i(k+1) = \mathbf{s}_i, \quad (8)$$

$i = 1, \ldots, L$.

Define the augmented state vector

$$\boldsymbol{x}(k) := \begin{bmatrix} \boldsymbol{x}_1(k) \\ \boldsymbol{x}_2(k) \\ x_3(k) \\ \vdots \\ x_{2+L}(k) \end{bmatrix} \in \mathbb{R}^{3+3+L}.$$

Discarding the original nonlinear output (1) and considering (8) instead allows to write the discrete-time linear system

$$\begin{cases} \boldsymbol{x}(k+1) = \boldsymbol{\mathcal{A}}(k)\,\boldsymbol{x}(k) + \boldsymbol{\mathcal{B}}(k)\,\mathbf{u}(k) \\ \boldsymbol{y}(k+1) = \boldsymbol{\mathcal{C}}(k+1)\,\boldsymbol{x}(k+1) \end{cases}, \quad (9)$$

where $\boldsymbol{\mathcal{A}}(k) \in \mathbb{R}^{(3+3+L)\times(3+3+L)}$,

$$\boldsymbol{\mathcal{A}}(k) := \begin{bmatrix} \mathbf{I} & T\mathbf{I} & \mathbf{0} \\ \mathbf{0} & \mathbf{I} & \mathbf{0} \\ \mathbf{0} & -T\mathbf{d}_1^T(k+1)\,\mathbf{R}^T(t_{k+1}) & \\ \vdots & \vdots & \boldsymbol{\mathcal{A}}_{33}(k) \\ \mathbf{0} & -T\mathbf{d}_L^T(k+1)\,\mathbf{R}^T(t_{k+1}) & \end{bmatrix},$$

$$\begin{aligned} \boldsymbol{\mathcal{A}}_{33}(k) := \operatorname{diag}\big(& \mathbf{d}_1^{\mathrm{T}}(\mathrm{k}+1)\,\mathbf{R}^{\mathrm{T}}(\mathrm{t}_{\mathrm{k}+1})\,\mathbf{R}(\mathrm{t}_{\mathrm{k}})\,\mathbf{d}_1(\mathrm{k}), \ldots, \\ & \mathbf{d}_L^T(k+1)\,\mathbf{R}^T(t_{k+1})\,\mathbf{R}(t_k)\,\mathbf{d}_L(k)\big), \end{aligned}$$

$$\boldsymbol{\mathcal{B}}(k) := \begin{bmatrix} \mathbf{I} \\ \mathbf{0} \\ -\mathbf{d}_1^T(k+1)\,\mathbf{R}^T(t_{k+1}) \\ \vdots \\ -\mathbf{d}_L^T(k+1)\,\mathbf{R}^T(t_{k+1}) \end{bmatrix} \in \mathbb{R}^{(3+3+L)\times 3},$$

and $\boldsymbol{\mathcal{C}}(k) \in \mathbb{R}^{3L\times(3+3+L)}$,

$$\boldsymbol{\mathcal{C}}(k) := \begin{bmatrix} \mathbf{I} & \mathbf{0} & \mathbf{R}(t_k)\,\mathbf{d}_1(k) & \mathbf{0} & \mathbf{0} \\ \vdots & \vdots & & \ddots & \\ \mathbf{I} & \mathbf{0} & \mathbf{0} & \mathbf{0} & \mathbf{R}(t_k)\,\mathbf{d}_L(k) \end{bmatrix}.$$

B. Observability analysis of the augmented system

The observability of the linear discrete-time system (9) is detailed in the following theorem.

Theorem 1: Suppose that, for some time $k_a \geq k_0$, there exist $i, j, l, m \in \{1, \ldots, L\}$ such that

$$\mathbf{d}_i(k_a) \neq \alpha_1 \mathbf{d}_j(k_a) \quad (10)$$

and

$$\mathbf{d}_l(k_a+1) \neq \alpha_2 \mathbf{d}_m(k_a+1) \quad (11)$$

for all $\alpha_1, \alpha_2 \in \mathbb{R}$. Then, the discrete-time linear system (9) is observable on $[k_a, k_a+2]$, i.e., the initial state $\mathbf{x}(k_a)$ is uniquely determined by the input $\{\mathbf{u}(k) : k = k_a, k_a+1\}$ and the output $\{\mathbf{y}(k) : k = k_a, k_a+1\}$.

Proof: The proof reduces to show that the observability matrix $\boldsymbol{\mathcal{O}}(k_a, k_a+2)$ associated with the pair $(\boldsymbol{\mathcal{A}}(k), \boldsymbol{\mathcal{C}}(k))$ on $[k_a, k_a+2]$, $k_a \geq k_0$, has rank equal to the number of states of the system. Fix $k_a \geq k_0$ and suppose that the rank of the observability matrix is less than the number of states of the system. Then, there exists a unit vector

$$\mathbf{c} = \begin{bmatrix} \mathbf{c}_1^T \\ \mathbf{c}_2^T \\ c_3 \\ \vdots \\ c_{2+L} \end{bmatrix} \in \mathbb{R}^{3+3+L},$$

with $\mathbf{c}_1, \mathbf{c}_2 \in \mathbb{R}^3$, $c_3, \ldots, c_{2+L} \in \mathbb{R}$, such that $\boldsymbol{\mathcal{O}}(k_a, k_a+2)\,\mathbf{c} = \mathbf{0}$ or, equivalently,

$$\begin{cases} \boldsymbol{\mathcal{C}}(k_a)\,\mathbf{c} = \mathbf{0} \\ \boldsymbol{\mathcal{C}}(k_a+1)\,\mathbf{A}(k_a)\,\mathbf{c} = \mathbf{0} \end{cases}. \quad (12)$$

Expanding the first equation of (12) gives

$$\left\{\begin{array}{l}\mathbf{c}_1+c_3\mathbf{R}\left(t_{k_a}\right)\mathbf{d}_1\left(k_a\right)=\mathbf{0}\\ \vdots\\ \mathbf{c}_1+c_{2+L}\mathbf{R}\left(t_{k_a}\right)\mathbf{d}_L\left(k_a\right)=\mathbf{0}\end{array}\right. . \tag{13}$$

Under the conditions of the theorem, there exist $i,j \in \{1,\ldots,L\}$ such that (10) holds for all α_1. Taking the difference between the i-th and the j-th equations of (13) gives

$$c_{2+i}\mathbf{R}\left(t_{k_a}\right)\mathbf{d}_i\left(k_a\right)-c_{2+j}\mathbf{R}\left(t_{k_a}\right)\mathbf{d}_j\left(k_a\right)=\mathbf{0}$$

or, equivalently,

$$c_{2+i}\mathbf{d}_i\left(k_i\right)-c_{2+j}\mathbf{d}_j\left(k_i\right)=\mathbf{0}. \tag{14}$$

If (10) holds for all α_1, then the only solution of (14) is

$$c_{2+i}=c_{2+j}=0. \tag{15}$$

In turn, substituting (15) in the i-th or the j-th equation of (13) allows to conclude that

$$\mathbf{c}_1=\mathbf{0}. \tag{16}$$

Then, substituting (16) in the remaining equations of (13) now gives

$$c_{2+1}=c_{2+2}=\ldots=c_{2+L}=0. \tag{17}$$

Now, substitute (16) and (17) in the second equation of (12), which allows to write

$$\left\{\begin{array}{l}T\left[\mathbf{I}-\mathbf{R}\left(t_{k_a+1}\right)\mathbf{d}_1\left(k_a+1\right)\mathbf{d}_1^T\left(k_a+1\right)\mathbf{R}^T\left(t_{k_a+1}\right)\right]\mathbf{c}_2=\mathbf{0}\\ \vdots\\ T\left[\mathbf{I}-\mathbf{R}\left(t_{k_a+1}\right)\mathbf{d}_L\left(k_a+1\right)\mathbf{d}_L^T\left(k_a+1\right)\mathbf{R}^T\left(t_{k_a+1}\right)\right]\mathbf{c}_2=\mathbf{0}\end{array}\right.$$

or, equivalently,

$$\left\{\begin{array}{l}\left[\mathbf{I}-\mathbf{d}_1\left(k_a+1\right)\mathbf{d}_1^T\left(k_a+1\right)\right]\mathbf{R}^T\left(t_{k_a+1}\right)\mathbf{c}_2=\mathbf{0}\\ \vdots\\ \left[\mathbf{I}-\mathbf{d}_L\left(k_a+1\right)\mathbf{d}_L^T\left(k_a+1\right)\right]\mathbf{R}^T\left(t_{k_a+1}\right)\mathbf{c}_2=\mathbf{0}\end{array}\right. . \tag{18}$$

Under the conditions of the theorem, (11) holds for all α_2, which in turn implies that the only solution of (18) is $\mathbf{c}_2=\mathbf{0}$. But this contradicts the hypothesis of existence of a unit vector $\mathbf{c}$ such that $\mathcal{O}\left(k_a,k_a+2\right)\mathbf{c}=\mathbf{0}$, which means that the observability matrix $\mathcal{O}\left(k_a,k_a+2\right)$ must have rank equal to the number of states of the system and as such the system is observable, which concludes the proof. ∎

C. Observability of the nonlinear system

In Section III-A a state augmentation procedure was presented that leads to a linear time-varying system that is related to the original nonlinear system. Its observability was characterized in Section III-B and now, in this section, its usefulness for the design of an estimation solution for the original nonlinear system is demonstrated. Sufficient conditions for the observability of the nonlinear system (3) are derived in the following theorem, which also relates the augmented system (9) with the nonlinear system (3).

Theorem 2: Suppose that the conditions of Theorem 1 hold for some $k_a \geq k_0$. Then:

i) the nonlinear system (3) is observable on the interval $[k_a,k_a+2]$ in the sense that the initial state $\{\mathbf{p}\left(t_{k_a}\right),\mathbf{v}_f\left(t_{k_a}\right)\}$ is uniquely determined by the input $\{\mathbf{u}\left(k\right):k=k_a,k_a+1\}$ and the output $\{\mathbf{d}_1\left(k\right),\ldots,\mathbf{d}_L\left(k\right):k=k_a,k_a+1\}$; and
ii) the initial condition of the augmented system (9) matches that of (3), i.e.,

$$\left\{\begin{array}{l}\boldsymbol{x}_1\left(k_a\right)=\mathbf{p}\left(t_{k_a}\right)\\ \boldsymbol{x}_2\left(k_a\right)=\mathbf{v}_f\left(t_{k_a}\right)\\ x_3\left(k_a\right)=\left\|\mathbf{s}_1-\mathbf{p}\left(t_{k_a}\right)\right\|\\ \vdots\\ x_{2+L}\left(k_a\right)=\left\|\mathbf{s}_L-\mathbf{p}\left(t_{k_a}\right)\right\|\end{array}\right. .$$

Proof: Let

$$\boldsymbol{x}\left(k_a\right):=\left[\begin{array}{c}\boldsymbol{x}_1\left(k_a\right)\\ \boldsymbol{x}_2\left(k_a\right)\\ x_3\left(k_a\right)\\ \vdots\\ x_{2+L}\left(k_a\right)\end{array}\right]\in\mathbb{R}^{3+3+L}$$

be the initial condition of (9) and let $\mathbf{p}\left(t_{k_a}\right)$ and $\mathbf{v}_f\left(t_{k_a}\right)$ be the initial condition of (3). From the output of (9) for $k=k_a$ it must be

$$\left\{\begin{array}{l}\boldsymbol{x}_1\left(k_a\right)+x_3\left(k_a\right)\mathbf{R}\left(t_{k_a}\right)\mathbf{d}_1\left(k_a\right)=\mathbf{s}_1\\ \vdots\\ \boldsymbol{x}_1\left(k_a\right)+x_{2+L}\left(k_a\right)\mathbf{R}\left(t_{k_a}\right)\mathbf{d}_L\left(k_a\right)=\mathbf{s}_L\end{array}\right. \tag{19}$$

and from the output of (3) for $k=k_a$ it must be

$$\left\{\begin{array}{l}\mathbf{d}_1\left(k_a\right)=\mathbf{R}^T\left(t_{k_a}\right)\frac{\mathbf{s}_1-\mathbf{p}\left(t_{k_a}\right)}{\left\|\mathbf{s}_1-\mathbf{p}\left(t_{k_a}\right)\right\|}\\ \vdots\\ \mathbf{d}_L\left(k_a\right)=\mathbf{R}^T\left(t_{k_a}\right)\frac{\mathbf{s}_L-\mathbf{p}\left(t_{k_a}\right)}{\left\|\mathbf{s}_L-\mathbf{p}\left(t_{k_a}\right)\right\|}\end{array}\right. . \tag{20}$$

Rearrange (20) as

$$\left\{\begin{array}{l}\mathbf{p}\left(t_{k_a}\right)+\left\|\mathbf{s}_1-\mathbf{p}\left(t_{k_a}\right)\right\|\mathbf{R}\left(t_{k_a}\right)\mathbf{d}_1\left(k_a\right)=\mathbf{s}_1\\ \vdots\\ \mathbf{p}\left(t_{k_a}\right)+\left\|\mathbf{s}_L-\mathbf{p}\left(t_{k_a}\right)\right\|\mathbf{R}\left(t_{k_a}\right)\mathbf{d}_L\left(k_a\right)=\mathbf{s}_L\end{array}\right. . \tag{21}$$

Under the conditions of the theorem (10) holds for all α_1. Taking the differences between the i-th and the j-th equations of both (19) and (21) and comparing the results yields

$$\begin{array}{r}\left[x_{2+i}\left(k_a\right)-\left\|\mathbf{s}_i-\mathbf{p}\left(t_{k_a}\right)\right\|\right]\mathbf{R}\left(t_{k_a}\right)\mathbf{d}_i\left(k_a\right)\\ -\left[x_{2+j}\left(k_a\right)-\left\|\mathbf{s}_j-\mathbf{p}\left(t_{k_a}\right)\right\|\right]\mathbf{R}\left(t_{k_a}\right)\mathbf{d}_j\left(k_a\right)=\mathbf{0}\end{array}$$

or, equivalently,

$$\begin{array}{r}\left[x_{2+i}\left(k_a\right)-\left\|\mathbf{s}_i-\mathbf{p}\left(t_{k_a}\right)\right\|\right]\mathbf{d}_i\left(k_a\right)\\ -\left[x_{2+j}\left(k_a\right)-\left\|\mathbf{s}_j-\mathbf{p}\left(t_{k_a}\right)\right\|\right]\mathbf{d}_j\left(k_a\right)=\mathbf{0}.\end{array} \tag{22}$$

As (10) holds for all α_1, it follows from (22) that it must be

$$\left\{\begin{array}{l}x_{2+i}\left(k_a\right)=\left\|\mathbf{s}_i-\mathbf{p}\left(t_{k_a}\right)\right\|\\ x_{2+j}\left(k_a\right)=\left\|\mathbf{s}_j-\mathbf{p}\left(t_{k_a}\right)\right\|\end{array}\right. . \tag{23}$$

Now, comparing the i-th (or the j-th) equations of (19) and (21), and using (23), allows to conclude that it must be

$$\boldsymbol{x}_1\left(k_a\right)=\mathbf{p}\left(t_{k_a}\right). \tag{24}$$

Using (24) and comparing (19) with (21) allows one to conclude that

$$\left\{\begin{array}{l} x_3\left(k_a\right)=\left\|\mathbf{s}_1-\mathbf{p}\left(t_{k_a}\right)\right\| \\ \vdots \\ x_{2+L}\left(k_a\right)=\left\|\mathbf{s}_L-\mathbf{p}\left(t_{k_a}\right)\right\| \end{array}\right. . \tag{25}$$

Now, compute the output of the linear system (9) for $k=k_a+1$ as a function of its initial state, which gives

$$\begin{gathered} \boldsymbol{x}_1\left(k_a\right)+T\boldsymbol{x}_2\left(k_a\right)+\mathbf{u}\left(k_a\right) \\ -T\mathbf{d}_i^T\left(k_a+1\right)\mathbf{R}^T\left(t_{k_a+1}\right)\boldsymbol{x}_2\left(k_a\right)\mathbf{R}\left(t_{k_a+1}\right)\mathbf{d}_i\left(k_a+1\right) \\ +\mathbf{d}_i^T\left(k_a+1\right)\mathbf{R}^T\left(t_{k_a+1}\right)\mathbf{R}\left(t_{k_a}\right)\mathbf{d}_i\left(k_a\right)x_{2+i}\left(k_a\right) \\ \mathbf{R}\left(t_{k_a+1}\right)\mathbf{d}_i\left(k_a+1\right) \\ -\mathbf{d}_i^T\left(k_a+1\right)\mathbf{R}^T\left(t_{k_a+1}\right)\mathbf{u}\left(k_a\right)\mathbf{R}\left(t_{k_a+1}\right)\mathbf{d}_i\left(k_a+1\right)=\mathbf{s}_i \end{gathered} \tag{26}$$

for all $i\in\{1,\ldots,L\}$. To compute the output of the nonlinear system (3) for $k=k_a+1$ as a function of its initial state write first

$$\mathbf{d}_i\left(k_a+1\right)=\mathbf{R}^T\left(t_{k_a+1}\right)\frac{\mathbf{s}_i-\mathbf{p}\left(t_{k_a}\right)-T\mathbf{v}_f\left(t_{k_a}\right)-\mathbf{u}\left(k_a\right)}{\left\|\mathbf{s}_i-\mathbf{p}\left(t_{k_a+1}\right)\right\|} \tag{27}$$

for all $i\in\{1,\ldots,L\}$. Rearrange (27) as

$$\begin{gathered} \mathbf{p}\left(t_{k_a}\right)+T\mathbf{v}_f\left(t_{k_a}\right)+\mathbf{u}\left(k_a\right) \\ +\left\|\mathbf{s}_i-\mathbf{p}\left(t_{k_a+1}\right)\right\|\mathbf{R}\left(t_{k_a+1}\right)\mathbf{d}_i\left(k_a+1\right)=\mathbf{s}_i \end{gathered} \tag{28}$$

for all $i\in\{1,\ldots,L\}$. Following the reasoning used to derive (7), one can express $\left\|\mathbf{s}_i-\mathbf{p}\left(t_{k_a+1}\right)\right\|$ as

$$\begin{gathered} \left\|\mathbf{s}_i-\mathbf{p}\left(t_{k_a+1}\right)\right\|=-T\mathbf{d}_i^T\left(k_a+1\right)\mathbf{R}^T\left(t_{k_a+1}\right)\mathbf{v}_f\left(t_{k_a}\right) \\ +\mathbf{d}_i^T\left(k_a+1\right)\mathbf{R}^T\left(t_{k_a+1}\right)\mathbf{R}\left(t_{k_a}\right)\mathbf{d}_i\left(k_a\right)\left\|\mathbf{s}_i-\mathbf{p}\left(t_{k_a}\right)\right\| \\ -\mathbf{d}_i^T\left(k_a+1\right)\mathbf{R}^T\left(t_{k_a+1}\right)\mathbf{u}\left(k_a\right) \end{gathered}$$

for all $i\in\{1,\ldots,L\}$. Substituting that in (28) yields

$$\begin{gathered} \mathbf{p}\left(t_{k_a}\right)+T\mathbf{v}_f\left(t_{k_a}\right)+\mathbf{u}\left(k_a\right) \\ -T\mathbf{d}_i^T\left(k_a+1\right)\mathbf{R}^T\left(t_{k_a+1}\right)\mathbf{v}_f\left(t_{k_a}\right)\mathbf{R}\left(t_{k_a+1}\right)\mathbf{d}_i\left(k_a+1\right) \\ +\mathbf{d}_i^T\left(k_a+1\right)\mathbf{R}^T\left(t_{k_a+1}\right)\mathbf{R}\left(t_{k_a}\right)\mathbf{d}_i\left(k_a\right) \\ \left\|\mathbf{s}_i-\mathbf{p}\left(t_{k_a}\right)\right\|\mathbf{R}\left(t_{k_a+1}\right)\mathbf{d}_i\left(k_a+1\right) \\ -\mathbf{d}_i^T\left(k_a+1\right)\mathbf{R}^T\left(t_{k_a+1}\right)\mathbf{u}\left(k_a\right)\mathbf{R}\left(t_{k_a+1}\right)\mathbf{d}_i\left(k_a+1\right)=\mathbf{s}_i \end{gathered} \tag{29}$$

for all $i\in\{1,\ldots,L\}$. Now, comparing (26) with (29) and using (24) and (25) allow to conclude that

$$\begin{gathered} T\left[\mathbf{I}-\mathbf{R}\left(t_{k_a+1}\right)\mathbf{d}_i\left(k_a+1\right)\mathbf{d}_i^T\left(k_a+1\right)\mathbf{R}^T\left(t_{k_a+1}\right)\right] \\ \left[\mathbf{v}_f\left(t_{k_a}\right)-\boldsymbol{x}_2\left(k_a\right)\right]=\mathbf{0} \end{gathered}$$

for all $i\in\{1,\ldots,L\}$ or, equivalently,

$$\begin{gathered} \left[\mathbf{I}-\mathbf{d}_i\left(k_a+1\right)\mathbf{d}_i^T\left(k_a+1\right)\right]\mathbf{R}^T\left(t_{k_a+1}\right) \\ \left[\mathbf{v}_f\left(t_{k_a}\right)-\boldsymbol{x}_2\left(k_a\right)\right]=\mathbf{0} \end{gathered} \tag{30}$$

for all $i\in\{1,\ldots,L\}$. Under the conditions of the theorem, (11) holds for all α_2, which in turn implies that the only solution of (30) is $\boldsymbol{x}_2\left(k_a\right)=\mathbf{v}_f\left(t_{k_a}\right)$. This concludes the second part of the theorem, as it has been shown that, in the conditions of the theorem, the initial condition of (3) corresponds to that of (9). Now, notice that, using Theorem 1, the initial condition of (9) is uniquely determined. As, in addition, the two initial conditions match, it follows that the initial condition of (3) is also uniquely determined, thus concluding the theorem. ∎

Theorem 2 presents only sufficient observability conditions. In the following theorem these are shown to be necessary if the same interval length is considered.

Theorem 3: The nonlinear system (3) is observable on $[k_a,k_a+2]$, in the sense that the initial state $\{\mathbf{p}\left(t_{k_a}\right),\mathbf{v}_f\left(t_{k_a}\right)\}$ is uniquely determined by the input $\{\mathbf{u}(k):k=k_a,k_a+1\}$ and the output $\{\mathbf{d}_1(k),\ldots,\mathbf{d}_L(k):k=k_a,k_a+1\}$, if and only if the conditions of Theorem 2 hold.

Proof: See Appendix A. ∎

Remark 1: In short, the observability conditions derived in the paper amount to say that, if there are two consecutive instants such that there are two noncollinear bearing measurements on each instant, then the system is observable. Three important situations should be considered in what concerns the number and configuration of landmarks: i) if there are at least three noncollinear landmarks, which is a realistic and typical scenario, the system is always observable, as there are always at least two noncollinear bearing measurements; ii) if two landmarks are available, the system is observable if the vehicle stays away from the line formed by the two landmarks; and iii) if there is only one landmark, observability may still be achieved over a longer period; this case falls out of the scope of the paper and it has been treated in [21].

D. Filter design

The results presented in the previous section are constructive in the sense that the design of an estimator for (3) can be obtained by designing an estimator for the linear discrete-time system (9). This yields estimates, in discrete time, of the position of the vehicle and the velocity of the fluid. As all the required quantities are available to obtain estimates of these quantities in continuous-time by open-loop propagation, between discrete-time updates one may use

$$\left\{\begin{array}{l} \hat{\mathbf{p}}(t)=\hat{\mathbf{p}}\left(t_k\right)+\left(t-t_k\right)\hat{\mathbf{v}}_f\left(t_k\right)+\int_{t_k}^t\mathbf{R}(\tau)\mathbf{v}_r(\tau)d\tau \\ \hat{\mathbf{v}}_f(t)=\hat{\mathbf{v}}_f\left(t_k\right) \end{array}\right. , \tag{31}$$

$t_k<t<t_{k+1}$.

IV. Filter design without state augmentation

This section presents an alternative method to estimate the position of the vehicle and the velocity of the fluid that does not require state augmentation. In short, a different artificial output, which is linear in the system state, is obtained and it is shown that its information suffices to retrieve the state of the system.

In order to construct an artificial output, notice first that as $\mathbf{d}_i$, $i=1,\ldots,L$, are unit vectors, one has that

$$\begin{gathered} \mathbf{d}_i(k)-\left(\mathbf{d}_i^T(k)\mathbf{d}_i(k)\right)\mathbf{d}_i(k)= \\ \left[\mathbf{I}-\mathbf{d}_i(k)\mathbf{d}_i^T(k)\right]\mathbf{d}_i(k)=\mathbf{0}. \end{gathered} \tag{32}$$

Substituting (1) in (32) allows to write

$$\left[\mathbf{I}-\mathbf{d}_i(k)\mathbf{d}_i^T(k)\right]\mathbf{R}^T\left(t_k\right)\frac{\mathbf{s}_i-\mathbf{p}\left(t_k\right)}{\left\|\mathbf{s}_i-\mathbf{p}\left(t_k\right)\right\|}=\mathbf{0},$$

which allows to express an artificial linear output as

$$\left[\mathbf{I}-\mathbf{d}_i(k)\mathbf{d}_i^T(k)\right]\mathbf{R}^T\left(t_k\right)\mathbf{p}\left(t_k\right)=$$
$$\left[\mathbf{I}-\mathbf{d}_i(k)\mathbf{d}_i^T(k)\right]\mathbf{R}^T\left(t_k\right)\mathbf{s}_i$$

for all $i \in \{1,\dots L\}$.

The solution proposed in this sections consists in replacing the nonlinear outputs of (3) with (33), which gives the linear system

$$\begin{cases} \begin{bmatrix} \mathbf{p}\left(t_{k+1}\right) \\ \mathbf{v}_f\left(t_{k+1}\right) \end{bmatrix} = \mathbf{A}(k) \begin{bmatrix} \mathbf{p}\left(t_k\right) \\ \mathbf{v}_f\left(t_k\right) \end{bmatrix} + \mathbf{B}\mathbf{u}(k) \\ \mathbf{y}(k) = \mathbf{C}(k) \begin{bmatrix} \mathbf{p}\left(t_k\right) \\ \mathbf{v}_f\left(t_k\right) \end{bmatrix} \end{cases}, \quad (33)$$

where

$$\mathbf{A}(k)=\begin{bmatrix} \mathbf{I} & T\mathbf{I} \\ \mathbf{0} & \mathbf{I} \end{bmatrix} \in \mathbb{R}^{6\times 6}, \quad \mathbf{B}=\begin{bmatrix} \mathbf{I} \\ \mathbf{0} \end{bmatrix} \in \mathbb{R}^{6\times 3},$$

and

$$\mathbf{C}(k)=\begin{bmatrix} \left[\mathbf{I}-\mathbf{d}_1(k)\mathbf{d}_1^T(k)\right]\mathbf{R}^T\left(t_k\right) & \mathbf{0} \\ \vdots & \vdots \\ \left[\mathbf{I}-\mathbf{d}_L(k)\mathbf{d}_L^T(k)\right]\mathbf{R}^T\left(t_k\right) & \mathbf{0} \end{bmatrix} \in \mathbb{R}^{3L\times 6}.$$

The following theorem addresses the observability of (33).

Theorem 4: The discrete-time linear sytem (33) is observable on $[k_a, k_a+2]$, i.e., the initial state $\{\mathbf{p}\left(t_{k_a}\right), \mathbf{v}_f\left(t_{k_a}\right)\}$ is uniquely determined by the input $\{\mathbf{u}\left(k\right): k=k_a, k_a+1\}$ and the output $\{\mathbf{y}\left(k\right): k=k_a, k_a+1\}$, if and only if the conditions of Theorem 1 hold.

Proof: See Appendix B. ■

The filter design follows as in Section III-D, only now an estimator is designed, in discrete-time, for the discrete-time linear system (33), whereas the open-loop propagation is given by (31).

V. Simulation results

Numerical simulations are presented and discussed in this section in order to evaluate the achievable performance with the proposed solutions for navigation based on multiple bearing measurements. First, the setup that is considered in the simulations is described in Section V-A. In order to evaluate the performance of the proposed solutions, the Bayesian Cramér-Rao Bound, briefly described in Section V-B, is computed. The two different proposed solutions will be detailed in Sections V-C and V-D. Finally, Monte Carlo results will be discussed in Section V-E.

A. Setup

In the simulations, an autonomous underwater vehicle is considered moving in the presence of ocean currents. The initial position of the vehicle was set to $\mathbf{p}(0) = [0\,0\,10]^T$ m, while the ocean current velocity was set to $\mathbf{v}_c(t) = [0.1\ -0.2\,0]^T$ m/s. The trajectory that is described by the vehicle is shown in Fig. 1. The vehicle is assumed to measure the bearings to a set of three landmarks, whose inertial positions are $\mathbf{s}_1 = \begin{bmatrix} 0 & 0 & 0 \end{bmatrix}^T$ (m), $\mathbf{s}_2 = \begin{bmatrix} 500 & 0 & 100 \end{bmatrix}$ (m), and $\mathbf{s}_3 = \begin{bmatrix} 0 & 500 & 100 \end{bmatrix}$ (m). Hence, as three noncolinear landmarks are available, the system is observable.

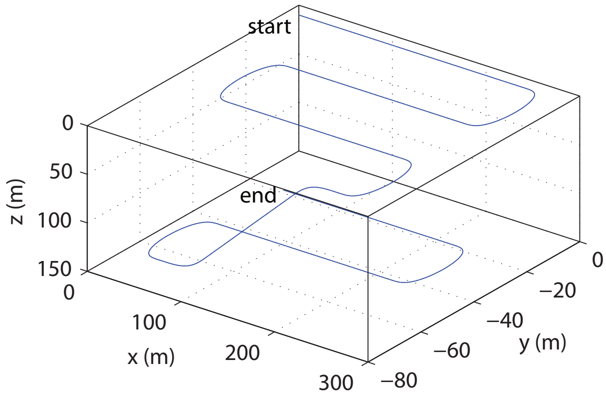

Fig. 1. Trajectory described by the vehicle

Inclination and azimuth angles to each of the landmarks are assumed to be measured. Hence, the directions are obtained from

$$\mathbf{d}_i = \begin{bmatrix} \sin\left(\theta_i\right)\cos\left(\varphi_i\right) \\ \sin\left(\theta_i\right)\sin\left(\varphi_i\right) \\ \cos\left(\theta_i\right) \end{bmatrix}, \; i=1,2,3,$$

where θ_i and φ_i are the inclination and azimuth angles to the i-th landmark, respectively. A sampling period of $T = 1$ s is considered for these angle measurements, and zero-mean Gaussian noise, with standard deviation of $1°$, was also added. The vehicle relative velocity, measured by a Doppler velocity log, is assumed available at 100 Hz and it is corrupted by additive zero-mean Gaussian noise, with standard deviation of $0.01\,\mathrm{m/s}$. The attitude, provided by an AHRS, available at 100 Hz, and parameterized by roll, pitch, and yaw Euler angles, is also assumed to be corrupted by zero-mean, additive Gaussian noise, with standard deviation of $0.03°$ for the roll and pitch and $0.3°$ for the yaw.

The discrete time input $\mathbf{u}(k)$, corresponding to a definite integral, was approximated using the trapezoid rule, while the open-loop solution of the position and ocean current velocity estimates, between bearing measurements, was computed using the Euler method. In fact, as it also corresponds to a definite integral, it is equivalent to the application of the trapezoid rule.

B. Bayesian Cramér-Rao bound

Although the optimal design of estimators for nonlinear systems is still an open field of research, there exist some theoretical bounds on the achievable performance in some cases. In particular, for a discrete-time system with linear process and nonlinear output, considering additive white Gaussian noise, it is possible to compute the Bayesian Cramér-Rao Bound (BCRB), which provides a lower bound on the covariance matrix of any given causal (realizable) unbiased estimator [22].

Consider the general discrete-time system

$$\begin{cases} \mathbf{x}(k+1) = \mathbf{F}(k)\mathbf{x}(k) + \mathbf{B}(k)\mathbf{u}(k) + \mathbf{n}_x(k) \\ \mathbf{y}(k) = \mathbf{h}\left(\mathbf{x}(k)\right) + \mathbf{n}_y(k) \end{cases}, \quad (34)$$

where $\mathbf{x}(k)$ is the state vector, $\mathbf{u}(k)$ is a deterministic system input, $\mathbf{y}(k)$ is the system output, which depends on the state vector through the nonlinear function $\mathbf{h}\left(\mathbf{x}(k)\right)$, $\mathbf{n}_x(k)$ follows a zero-mean Gaussian distribution with covariance $\mathbf{Q}_x(k)$, and $\mathbf{n}_y(k)$ follows a zero-mean Gaussian distribution with covariance $\mathbf{Q}_y(k)$. The recursion that provides the BCRB is similar to that of the EKF, with the difference that the Jacobian of $\mathbf{h}\left(\mathbf{x}(k+1)\right)$ is evaluated at the true state, see [22, Section 2.3.3]. Using the information matrix representation, the BCRB lower bound $\mathbf{P}_L(k)$ is given by

$$\mathbf{P}_L(k) = \mathbf{J}^{-1}(k),$$

where $\mathbf{J}(k)$ satisfies the recursion

$$\mathbf{J}(k+1) = \left[\mathbf{Q}_x\left(k\right) + \mathbf{F}\left(k\right)\mathbf{J}^{-1}\left(k\right)\mathbf{F}^T\left(k\right)\right]^{-1} + \mathbf{P}_m\left(k+1\right),$$

where $\mathbf{P}_m\left(k+1\right)$ accounts for the covariance reduction due to the observations, given by

$$\mathbf{P}_m(k+1) = E_{\mathbf{x}(k+1)}\left\{\tilde{\mathbf{H}}^T(\mathbf{x}\left(k+1\right))\mathbf{Q}_y^{-1}(k+1)\tilde{\mathbf{H}}(\mathbf{x}\left(k+1\right))\right\}, \tag{35}$$

where $\tilde{\mathbf{H}}\left(\mathbf{x}\left(k+1\right)\right)$ is the Jacobian of the nonlinear observation function evaluated at $\mathbf{x}(k+1)$. The subscript m stands for measurement.

The expectation in (35) is computed with respect to the state vector $\mathbf{x}(k+1)$ and as such it is usually evaluated resorting to Monte Carlo simulations. In nonlinear estimation problems, as in this paper, it is often of interest to evaluate the performance along specific or nominal trajectories $\overline{\mathbf{x}}(k)$. In this case, the term $\mathbf{P}_m(k+1)$ can be simplified to

$$\mathbf{P}_m(k+1) = \tilde{\mathbf{H}}^T\left(\overline{\mathbf{x}}(k+1)\right)\mathbf{Q}_y^{-1}(k+1)\,\tilde{\mathbf{H}}\left(\overline{\mathbf{x}}(k+1)\right),$$

which allows the assessment of the achievable performance for any tracker or estimator given the specific underlying problem structure. The resulting equations are analogous to the information filter version of the extended Kalman Filter, whereas the Jacobians are computed at the nominal trajectories $\overline{\mathbf{x}}(k)$ instead of the estimated trajectories, as convincingly argued in [22].

Using inclination and azimuth angles, and considering additive noise in these angles, as well as in the relative velocity measurements, the discrete-time system (3) can be written in the form of (34) and hence one can compute the BCRB. This lower bound was computed and it is presented in the ensuing.

C. Filter with state augmentation

Following the results presented in Section III, a Kalman filter is applied to the augmented system (9), which yields globally exponentially stable error dynamics. To tune the Kalman filter, the state disturbance covariance matrix was chosen as $\operatorname{diag}\left(0.01^2\mathbf{I},\, 0.001^2\mathbf{I},\, 10\mathbf{I}\right)$ and the output noise covariance matrix was set to $10\mathbf{I}$. These values were chosen empirically to adjust the performance of the proposed solution with state augmentation.

The initial condition for the position was set $\hat{\mathbf{x}}_1(0) = \left[-1000\ -1000\ 100\right]^T\ (\mathrm{m})$, while the ocean current velocity was set to zero. The states corresponding to the ranges were also set to zero. In this way, the filter is initialized with large position and range errors. The initial covariance of the filter was set to $\operatorname{diag}\left(10^2\mathbf{I},\, \mathbf{I},\, \mathbf{I}\right)$.

The initial convergence of the position and velocity errors is depicted in Fig. 2. As it is possible to observe, the error converges very quickly to a neighborhood of zero (it does not converge to zero only due to the presence of sensor noise). The detailed evolutions of the position and velocity errors are

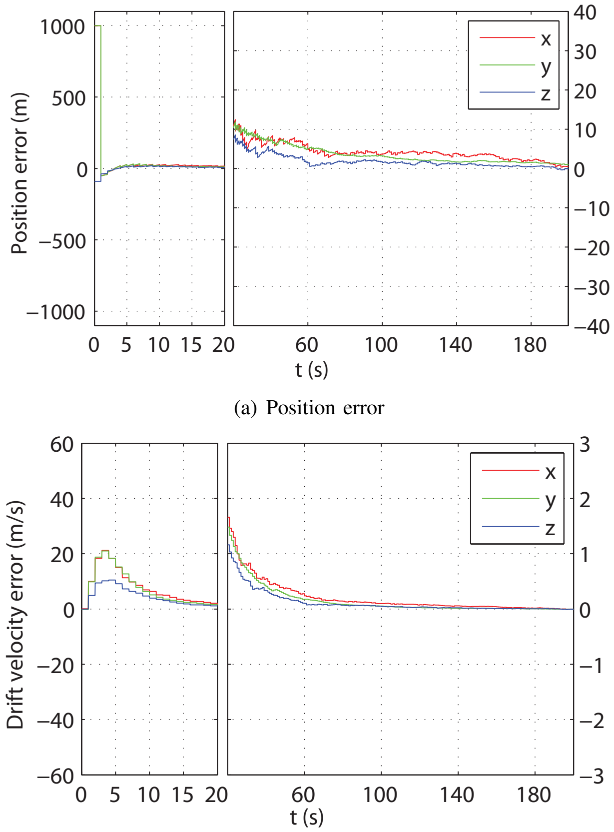

(a) Position error

(b) Ocean current velocity error

Fig. 2. Initial convergence of the errors (filter with state augmentation)

depicted in Fig. 3. In this plot, the one σ bounds obtained from the covariance of the Kalman filter (corresponding to the square root of the diagonal elements of the Kalman filter covariance matrix) are also depicted in dashed lines. Finally, the one σ BCRB bound (more specifically the square root of the diagonal elements of $\mathbf{P}_L(k)$) is also plotted in solid thicker lines. The most noticeable feature is that the position and velocity errors remain, most of the time, below $2\,\mathrm{m}$ and $0.02\,\mathrm{m/s}$, respectively. The achieved performance is mostly in agreement with the Bayesian Cramér-Rao lower bound, and it is also possible to observe that, sometimes, the filter is slightly overconfident, particularly along the x-coordinate of the position. For the sake of completeness, the evolution of the range errors is shown in Fig. 4.

D. Filter without state augmentation

In this section a Kalman filter is applied to the alternative system proposed in Section IV. To tune the Kalman filter, the state disturbance covariance matrix was chosen as $\operatorname{diag}\left(0.01^2\mathbf{I},\, 0.001^2\mathbf{I}\right)$ and the output noise covariance matrix was set to $10\mathbf{I}$. These values were chosen empirically to adjust the performance of the proposed solution without state

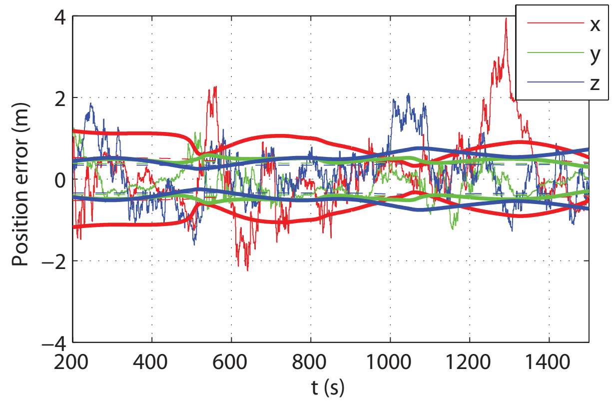

(a) Position error

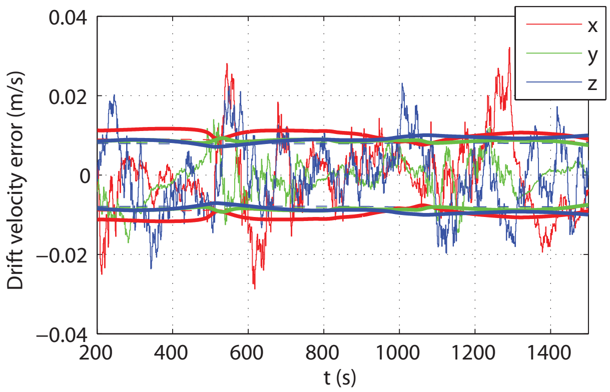

(b) Ocean current velocity error

Fig. 3. Steady-state evolution of the errors (filter with state augmentation)

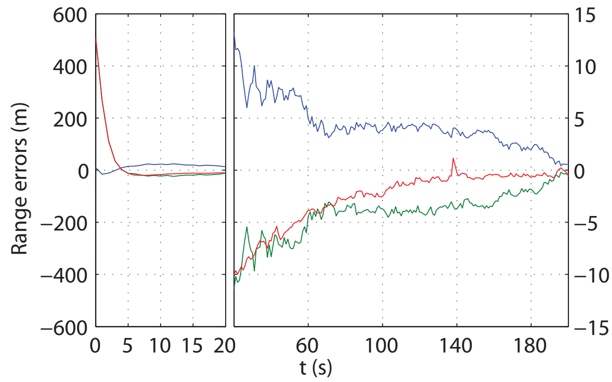

(a) Initial convergence

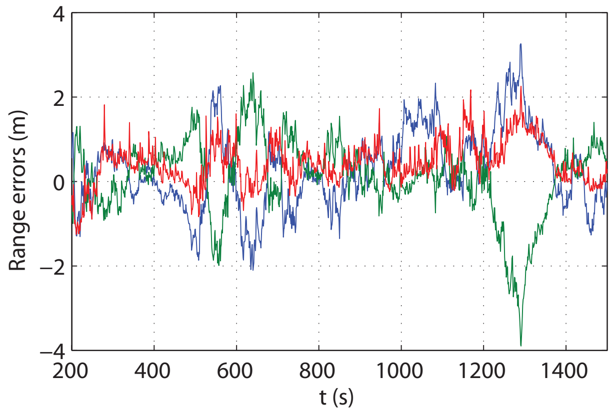

(b) Steady-state evolution

Fig. 4. Evolution of the range errors (filter with state augmentation)

augmentation. All initial conditions were set as before, only now there are no additional states corresponding to the ranges.

The initial convergence of the position and velocity errors is depicted in Fig. 5. As it is possible to observe, the error converges very quickly to a neighborhood of zero (it does not converge to zero only due to the presence of sensor noise). Comparing Fig. 2 with Fig. 5, one can conclude that the filter with state augmentation converges slightly slower than the one without state augmentation, which perhaps can be explained by the additional burden of also estimating the distances. The detailed evolutions of the position and velocity errors are depicted in Fig. 6, along with the one σ bounds obtained from the Kalman filter covariance matrix and the BCRB, just as in Fig. 3. The most noticeable feature is, again, that the position and velocity errors remain, most of the time, below $2\,\mathrm{m}$ and $0.02\,\mathrm{m/s}$, respectively. The steady-state performance is very similar to that obtained with the filter with state augmentation.

E. Performance comparison

The proposed solutions were compared with the extended Kalman filter applied to the original nonlinear system (3). The initial estimates were set as in the previous simulation. In order to achieve good performance, the state disturbance matrix was set to $\mathrm{diag}\left(0.01^2\mathbf{I},\, 0.001^2\mathbf{I}\right)$ and the output noise covariance matrix was set to $2 \times 10^{-5}\mathbf{I}$.

The initial convergence of the position and velocity errors is depicted in Fig. 7. In comparison with the proposed solutions, the extended Kalman filter exhibits a slightly slower convergence and much larger initial transients. The detailed evolutions of the position and velocity errors are depicted in Fig. 8, along with the one σ bounds obtained from the extended Kalman filter covariance matrix and the BCRB. The EKF performs, in steady-state, similarly to the proposed solutions. It does not offer, however, global convergence guarantees.

Finally, in order to better evaluate the performance of the proposed solutions, the Monte Carlo method was applied, and 1000 simulations were carried out with different, randomly generated noise signals. The standard deviation of the errors were computed in steady-state (for $t \geq 360$ s) for each simulation and averaged over the set of simulations. The results are depicted in Table I. The results with the EKF are also included. Additionally, the average steady-state one σ BCRB was computed (for $t \geq 360$ s), as shown in Table I. Comparing the performance of the proposed solutions, as well as that of the EKF, it is possible to observe that they are all very similar. Notice that the proposed solutions may achieve smaller standard deviation than the theoretical BCRB. This is so because the BCRB assumes an unbiased estimator, whereas the proposed solutions may be slightly biased, which is not uncommon in nonlinear estimation problems.

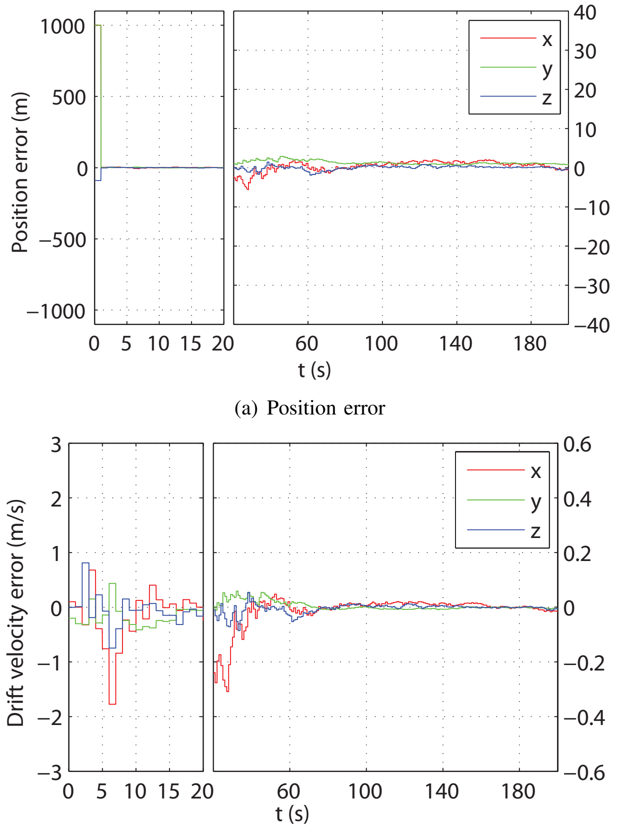

(a) Position error

(b) Ocean current velocity error

Fig. 5. Initial convergence of the errors (filter without state augmentation)

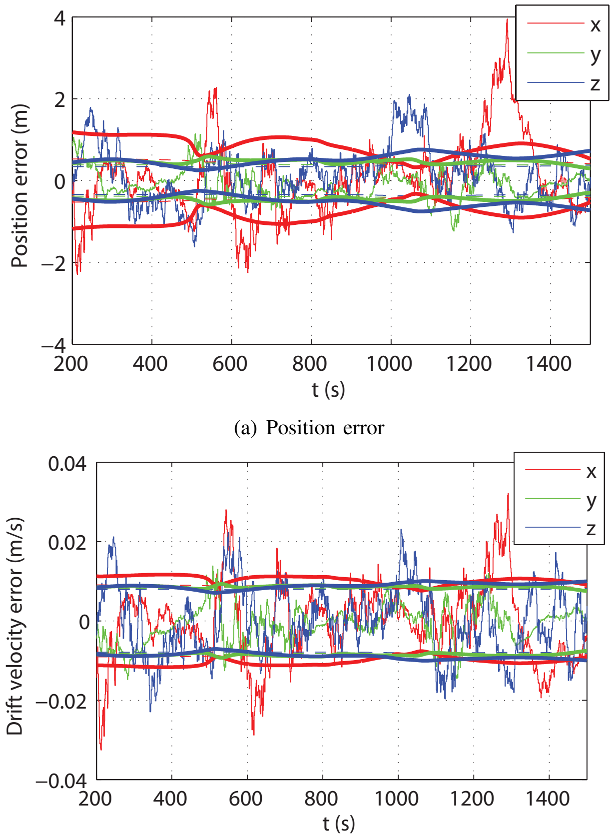

(a) Position error

(b) Ocean current velocity error

Fig. 6. Steady-state evolution of the errors (filter without state augmentation)

TABLE I
STANDARD DEVIATION OF THE STEADY-STATE ESTIMATION ERROR, AVERAGED OVER 1000 RUNS OF THE SIMULATION

Variable	Standard deviation with state augmentation	Standard deviation without state augmentation
$\tilde{\mathbf{p}}_x$ (m)	89.4×10^{-2}	89.4×10^{-2}
$\tilde{\mathbf{p}}_y$ (m)	41.5×10^{-2}	41.4×10^{-2}
$\tilde{\mathbf{p}}_z$ (m)	70.0×10^{-2}	70.7×10^{-2}
$\tilde{\mathbf{v}}_{fx}$ (m/s)	9.72×10^{-3}	9.72×10^{-3}
$\tilde{\mathbf{v}}_{fy}$ (m/s)	4.96×10^{-3}	5.00×10^{-3}
$\tilde{\mathbf{v}}_{fz}$ (m/s)	9.06×10^{-3}	9.06×10^{-3}

Variable	EKF standard deviation	Average BCRB
$\tilde{\mathbf{p}}_x$ (m)	88.4×10^{-2}	79.6×10^{-2}
$\tilde{\mathbf{p}}_y$ (m)	44.4×10^{-2}	46.2×10^{-2}
$\tilde{\mathbf{p}}_z$ (m)	65.0×10^{-2}	52.6×10^{-2}
$\tilde{\mathbf{v}}_{fx}$ (m/s)	12.2×10^{-3}	10.2×10^{-3}
$\tilde{\mathbf{v}}_{fy}$ (m/s)	8.37×10^{-3}	8.57×10^{-3}
$\tilde{\mathbf{v}}_{fz}$ (m/s)	11.9×10^{-3}	8.92×10^{-3}

VI. CONCLUSIONS

This paper addressed the problem of navigation based on multiple bearing measurements and two different solutions were proposed. First, the observability of the system was addressed and sufficient and necessary conditions were derived. The observability analyses were constructive and, in both cases, the discrete-time nature of the bearing measurements was taken into account and globally exponentially stable error dynamics are achieved with the design of estimators for linear systems. This is a result of appropriate state augmentation and output transformations that allow to consider linear systems for a problem that is, originally, nonlinear, without resorting to any kind of approximations. Simulation results were discussed, including a comparison with the extended Kalman filter and the Bayesian Cramér-Rao bound, as well as Monte Carlo runs. In short, the proposed filters achieve performances that are tight to the theoretical lower bound, and provide, at the same time, global convergence guarantees. In terms of computational complexity, the solution with state augmentation has more states than both the solution without state augmentation and the EKF, which have the same number of states.

REFERENCES

[1] S. Sukkarieh, E. Nebot, and H. Durrant-Whyte, "A high integrity IMU/GPS navigation loop for autonomous land vehicle applications," *IEEE Transactions on Robotics and Automation*, vol. 15, no. 3, pp. 572–578, Jun. 1999.

[2] L. Techy, K. Morgansen, and C. Woolsey, "Long-baseline acoustic localization of the Seaglider underwater glider," in *Proceedings of the 2011 American Control Conference*, San Francisco, USA, Jun.-Jul. 2011, pp. 3990–3995.

[3] L. Whitcomb, D. Yoerger, and H. Singh, "Combined Doppler/LBL Based Navigation of Underwater Vehicles," in *Proceedings of the 11th International Symposium on Unmanned Untethered Submersible Technology*, Durham, New Hampshire, USA, Aug. 1999, pp. 1–7.

[4] J. Vaganay, J. Bellingham, and J. Leonard, "Comparison of fix computation and filtering for autonomous acoustic navigation," *International Journal of Systems Science*, vol. 29, no. 10, pp. 1111–1122, Oct. 1998.

[5] J. Kinsey and L. Whitcomb, "Preliminary field experience with the DVLNAV integrated navigation system for manned and unmanned submersibles," in *Proceedings of the 1st IFAC Workshop on Guidance and Control of Underwater Vehicles*, Newport, South Wales, UK, Apr. 2003, pp. 83–88.

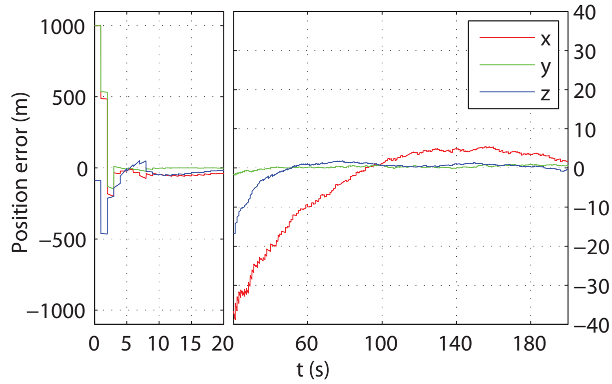

(a) Position error

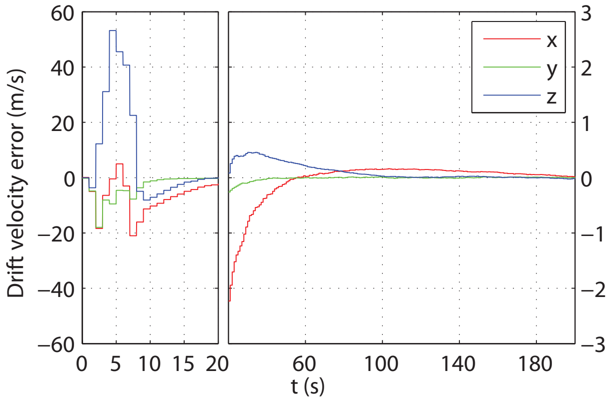

(b) Ocean current velocity error

Fig. 7. Initial convergence of the EKF errors

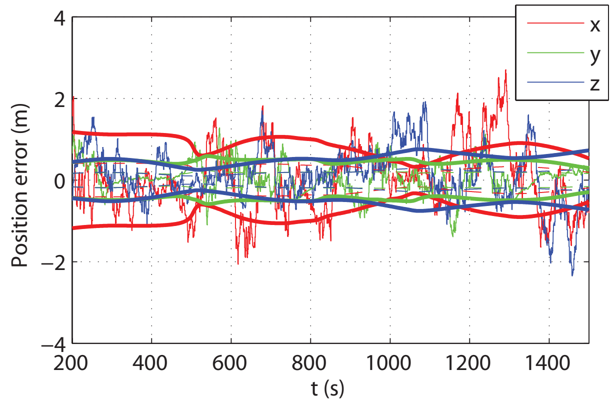

(a) Position error

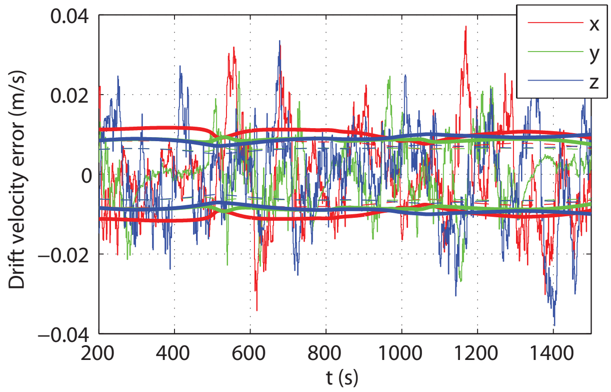

(b) Ocean current velocity error

Fig. 8. Steady-state evolution of the EKF errors

[6] J. Jouffroy and J. Opderbecke, "Underwater vehicle trajectory estimation using contracting PDE-based observers," in *Proceedings of the 2004 American Control Conference*, vol. 5, Boston, MA, USA, Jun-July 2004, pp. 4108–4113.

[7] G. Indiveri, P. Pedone, and M. Cuccovillo, "Fixed Target 3D Localization Based on Range Data Only: a Recursive Least Squares Approach," in *Proceedings of the 9th IFAC Conference on Manoeuvring and Control of Marine Craft*, Arenzano, Italy, Sep. 2012, pp. 1–6.

[8] A. Gadre and D. Stilwell, "A complete solution to underwater navigation in the presence of unknown currents based on range measurements from a single location," in *Proceedings of the 2005 IEEE/RSJ International Conference on Intelligent Robots and Systems*, Edmonton AB, Canada, Aug. 2005, pp. 1420–1425.

[9] J. Jouffroy and J. Reger, "An algebraic perspective to single-transponder underwater navigation," in *Proceedings of the 2006 IEEE International Conference on Control Applications*, Munich, Germany,, Oct. 2006, pp. 1789–1794.

[10] P.-M. Lee, B.-H. Jun, K. Kim, J. Lee, T. Aoki, and T. Hyakudome, "Simulation of an Inertial Acoustic Navigation System With Range Aiding for an Autonomous Underwater Vehicle," *IEEE Journal of Oceanic Engineering*, vol. 32, no. 2, pp. 327–345, Apr. 2007.

[11] P. Batista, C. Silvestre, and P. Oliveira, "Single Range Aided Navigation and Source Localization: observability and filter design," *Systems & Control Letters*, vol. 60, no. 8, pp. 665–673, Aug. 2011.

[12] M. Deghat, I. Shames, B. Anderson, and C. Yu, "Target Localization and Circumnavigation Using Bearing Measurements in 2D," in *Proceedings of the 49th IEEE Conference on Decision and Control*, Atlanta, GA., USA, Dec. 2010, pp. 334–339.

[13] S. Nardone and V. Aidala, "Observability Criteria for Bearings-Only Target Motion Analysis," *IEEE Transactions on Aerospace and Electronic Systems*, vol. 17, no. 2, pp. 162–166, Mar. 1981.

[14] S. Hammel and V. Aidala, "Observability Requirements for Three-Dimensional Tracking via Angle Measurements," *IEEE Transactions on Aerospace and Electronic Systems*, vol. 21, no. 2, pp. 200–207, Mar. 1985.

[15] K. Briechle and U. Hanebeck, "Localization of a Mobile Robot Using Relative Bearing Measurements," *IEEE Transactions on Robotics and Automation*, vol. 20, no. 1, pp. 36–44, Feb. 2004.

[16] J.-P. Cadre and C. Jauffret, "Discrete-Time Observability and Estimability Analysis for Bearings-Only Target Motion Analysis," *IEEE Transactions on Aerospace and Electronic Systems*, vol. 33, no. 1, pp. 178–201, Jan. 1997.

[17] T. Bréhard and J.-P. Cadre, "Closed-Form Posterior Cramér-Rao Bounds for Bearings-Only Tracking," *IEEE Transactions on Aerospace and Electronic Systems*, vol. 42, no. 4, pp. 1198–1223, Oct. 2006.

[18] ——, "Hierarchical Particle Filter for Bearings-Only Tracking," *IEEE Transactions on Aerospace and Electronic Systems*, vol. 43, no. 4, pp. 1567–1585, Oct. 2007.

[19] P. Leong, S. Arulampalam, T. Lamahewa, and T. Abhayapala, "A Gaussian-Sum Based Cubature Kalman Filter for Bearings-Only Tracking," *IEEE Transactions on Aerospace and Electronic Systems*, vol. 49, no. 2, pp. 1161–1176, Apr. 2013.

[20] P. Batista, C. Silvestre, and P. Oliveira, "Globally exponentially stable filters for source localization and navigation aided by direction measurements," *Systems & Control Letters*, vol. 62, no. 11, pp. 1065–1072, Nov. 2013.

[21] ——, "GES Source Localization and Navigation based on Discrete-Time Bearing Measurement," in *Proceedings of the 52nd IEEE Conference on Decision and Control*, Florence, Italy, Dec. 2013, pp. 5066–5071.

[22] H. L. Van Trees and K. L. Bell, *Bayesian Bounds for Parameter Estimation and Nonlinear Filtering/Tracking*. Piscataway, New Jersey, USA: IEEE Press, 2007.

Appendix A
Proof of Theorem 3

Proof: The sufficiency part is shown in Theorem 2 and as such only the necessity of the conditions needs to be established. Suppose first that (10) does not hold. That means that all directions are identical for $k = k_a$. Let $\mathbf{d}_i^u(k)$,

$k = k_a, k_a+1$, denote the output of the nonlinear system (3) with initial condition

$$\left\{ \begin{array}{l} \mathbf{p}^u(t_{k_a}) = \mathbf{p}^o \\ \mathbf{v}_f^u(t_{k_a}) = \mathbf{v}_s^o \end{array} \right.$$

and input $\mathbf{u}(k)$, $k = k_a, k_a+1$, i.e.

$$\left\{ \begin{array}{l} \mathbf{d}_i^u(k_a) = \frac{\mathbf{s}_i - \mathbf{p}^o}{\|\mathbf{s}_i - \mathbf{p}^o\|} =: \mathbf{d}^o \\ \mathbf{d}_i^u(k_a+1) = \frac{\mathbf{s}_i - \mathbf{p}^o - T\mathbf{v}_s^o - \mathbf{u}(k_a)}{\|\mathbf{s}_i - \mathbf{p}^o - T\mathbf{v}_s^o - \mathbf{u}(k_a)\|} \end{array} \right.$$

for all $i \in \{1, \ldots, L\}$. Consider a different initial condition

$$\left\{ \begin{array}{l} \mathbf{p}^v(t_{k_a}) = \mathbf{p}^o - \alpha \mathbf{d}^o \\ \mathbf{v}_f^v(t_{k_a}) = \mathbf{v}_s^o + \frac{\alpha}{T}\mathbf{d}^o \end{array} \right. ,$$

with $\alpha > 0$, and denote by $\mathbf{d}_i^v(k)$, $k = k_a, k_a+1$, the corresponding output for the same input. Then,

$$\begin{aligned} \mathbf{d}_i^v(k_a) &= \frac{\mathbf{s}_i - \mathbf{p}^o + \alpha\mathbf{d}^o}{\|\mathbf{s}_i - \mathbf{p}^o + \alpha\mathbf{d}^o\|} = \frac{(\|\mathbf{s}_i - \mathbf{p}^o\| + \alpha)\,\mathbf{d}^o}{\|(\|\mathbf{s}_i - \mathbf{p}^o\| + \alpha)\,\mathbf{d}^o\|} \\ &= \mathbf{d}^o = \mathbf{d}_i^u(k_a) \end{aligned}$$

and

$$\begin{aligned} \mathbf{d}_i^v(k_a+1) &= \frac{\mathbf{s}_i - \mathbf{p}^o + \alpha\mathbf{d}^o - T\mathbf{v}_s^o - \alpha\mathbf{d}^o - \mathbf{u}(k_a)}{\|\mathbf{s}_i - \mathbf{p}^o + \alpha\mathbf{d}^o - T\mathbf{v}_s^o - \alpha\mathbf{d}^o - \mathbf{u}(k_a)\|} \\ &= \frac{\mathbf{s}_i - \mathbf{p}^o - T\mathbf{v}_s^o - \mathbf{u}(k_a)}{\|\mathbf{s}_i - \mathbf{p}^o - T\mathbf{v}_s^o - \mathbf{u}(k_a)\|} = \mathbf{d}_i^u(k_a+1) \end{aligned}$$

for all $i \in \{1, \ldots L\}$. It has been shown that, if (10) does not hold, then there exist at least two initial conditions such that the system output is identical, which means that the nonlinear system (3) is not observable. Suppose now that (11) does not hold. That means that all directions are identical for $k = k_a+1$. Let $\mathbf{d}_i^u(k)$, $k = k_a, k_a+1$, denote the output of the nonlinear system (3) with initial condition

$$\left\{ \begin{array}{l} \mathbf{p}^u(t_{k_a}) = \mathbf{p}^o \\ \mathbf{v}_f^u(t_{k_a}) = \mathbf{v}_s^o \end{array} \right.$$

and input $\mathbf{u}(k)$, $k = k_a, k_a+1$, i.e.

$$\left\{ \begin{array}{l} \mathbf{d}_i^u(k_a) = \frac{\mathbf{s}_i - \mathbf{p}^o}{\|\mathbf{s}_i - \mathbf{p}^o\|} \\ \mathbf{d}_i^u(k_a+1) = \frac{\mathbf{s}_i - \mathbf{p}^o - T\mathbf{v}_s^o - \mathbf{u}(k_a)}{\|\mathbf{s}_i - \mathbf{p}^o - T\mathbf{v}_s^o - \mathbf{u}(k_a)\|} =: \mathbf{d}^o \end{array} \right.$$

for all $i \in \{1, \ldots, L\}$. Consider a different initial condition

$$\left\{ \begin{array}{l} \mathbf{p}^v(t_{k_a}) = \mathbf{p}^o \\ \mathbf{v}_f^v(t_{k_a}) = \mathbf{v}_s^o - \frac{\alpha}{T}\mathbf{d}^o \end{array} \right. ,$$

with $\alpha > 0$, and denote by $\mathbf{d}_i^v(k)$, $k = k_a, k_a+1$, the corresponding output for the same input. Then,

$$\mathbf{d}_i^v(k_a) = \frac{\mathbf{s}_i - \mathbf{p}^o}{\|\mathbf{s}_i - \mathbf{p}^o\|} = \mathbf{d}_i^u(k_a)$$

and

$$\begin{aligned} \mathbf{d}_i^v(k_a+1) &= \frac{\mathbf{s}_i - \mathbf{p}^o - T\mathbf{v}_s^o + \alpha\mathbf{d}^o - \mathbf{u}(k_a)}{\|\mathbf{s}_i - \mathbf{p}^o - T\mathbf{v}_s^o + \alpha\mathbf{d}^o - \mathbf{u}(k_a)\|} \\ &= \frac{(\|\mathbf{s}_i - \mathbf{p}^o - T\mathbf{v}_s^o - \mathbf{u}(k_a)\| + \alpha)\,\mathbf{d}^o}{\|(\|\mathbf{s}_i - \mathbf{p}^o - T\mathbf{v}_s^o - \mathbf{u}(k_a)\| + \alpha)\,\mathbf{d}^o\|} \\ &= \mathbf{d}^o = \mathbf{d}_i^u(k_a+1) \end{aligned}$$

for all $i \in \{1, \ldots L\}$. It has been shown that, if (11) does not hold, then there exist at least two initial conditions such that the system output is identical, which means that the nonlinear system (3) is not observable. This concludes the proof, as it has been shown that if either (10) or (11) do not hold, than the system is not observable and thus both conditions are necessary for the nonlinear system (3) to be observable. ■

Appendix B
Proof of Theorem 4

Proof: The proof amounts to show that the observability matrix $\boldsymbol{O}(k_a, k_a+2)$ associated with the pair $(\mathbf{A}(k), \mathbf{C}(k))$ on $[k_a, k_a+2]$ has rank equal to the number of states of the system if and only if both (10) and (11) hold for some $i, j, l, m \in \{1, \ldots, L\}$. Suppose that the system is not observable and both (10) and (11) hold for some $i, j, l, m \in \{1, \ldots, L\}$. Then, there exists a unit vector

$$\mathbf{c} = \left[\begin{array}{c} \mathbf{c}_1 \\ \mathbf{c}_2 \end{array} \right] \in \mathbb{R}^6, \; \mathbf{c}_1, \mathbf{c}_2 \in \mathbb{R}^3,$$

such that $\boldsymbol{O}(k_a, k_a+2)\,\mathbf{c} = \mathbf{0}$ or, equivalently,

$$\left\{ \begin{array}{l} \mathbf{C}(k_a)\,\mathbf{c} = \mathbf{0} \\ \mathbf{C}(k_a+1)\,\mathbf{A}(k_a)\,\mathbf{c} = \mathbf{0} \end{array} \right. . \tag{36}$$

From the first equation of (36) one has that

$$\left\{ \begin{array}{l} \left[\mathbf{I} - \mathbf{d}_1(k_a)\,\mathbf{d}_1^T(k_a)\right]\mathbf{R}^T(t_{k_a})\,\mathbf{c}_1 = \mathbf{0} \\ \vdots \\ \left[\mathbf{I} - \mathbf{d}_L(k_a)\,\mathbf{d}_L^T(k_a)\right]\mathbf{R}^T(t_{k_a})\,\mathbf{c}_1 = \mathbf{0} \end{array} \right. . \tag{37}$$

If (10) holds for some $i, j \in \{1, \ldots, L\}$, then the only solution of (37) is $\mathbf{c}_1 = \mathbf{0}$. Substituting that in the second equation of (36) gives

$$\left\{ \begin{array}{l} T\left[\mathbf{I} - \mathbf{d}_1(k_a+1)\,\mathbf{d}_1^T(k_a+1)\right]\mathbf{R}^T(t_{k_a+1})\,\mathbf{c}_2 = \mathbf{0} \\ \vdots \\ T\left[\mathbf{I} - \mathbf{d}_L(k_a+1)\,\mathbf{d}_L^T(k_a+1)\right]\mathbf{R}^T(t_{k_a+1})\,\mathbf{c}_2 = \mathbf{0} \end{array} \right. . \tag{38}$$

As (11) is assumed to hold for some $l, m \in \{1, \ldots, L\}$, then the only solution of (38) is $\mathbf{c}_2 = \mathbf{0}$. But this contradicts the hypothesis of existence of a unit vector $\mathbf{c}$ such that (36) holds. Then, if both (10) and (11) hold for some $i, j, l, m \in \{1, \ldots, L\}$, then the system is observable, thus concluding the proof of sufficiency. To show necessity, suppose first that (10) is not verified. Then, for $k = k_a$, all directions are identical. Let $\mathbf{d}_i(k_a) = \mathbf{d}^o$ for all $i = 1, \ldots, L$ and let

$$\mathbf{c} = \left[\begin{array}{c} \mathbf{R}(t_{k_a})\,\mathbf{d}^o \\ \mathbf{0} \end{array} \right].$$

Then, $\boldsymbol{O}(k_a, k_a+2)\,\mathbf{c} = \mathbf{0}$, which means that the system is not observable. Suppose now that (11) is not verified. Then, for $k = k_a+1$, all directions are identical. Let $\mathbf{d}_i(k_a+1) = \mathbf{d}^o$ for all $i = 1, \ldots, L$ and let

$$\mathbf{c} = \left[\begin{array}{c} \mathbf{0} \\ \mathbf{R}(t_{k_a+1})\,\mathbf{d}^o \end{array} \right].$$

Then, $\boldsymbol{O}(k_a, k_a+2)\,\mathbf{c} = \mathbf{0}$, which means that the system is not observable. Therefore, if either (10) or (11) are not verified, the system (33) is not observable, which implies that if (33) is observable, then both (10) and (11) must hold, therefore concluding the proof of necessity. ■

Pedro Batista (M'10) received the Licenciatura degree in Electrical and Computer Engineering in 2005 and the Ph.D. degree in 2010, both from Instituto Superior Técnico (IST), Lisbon, Portugal. From 2004 to 2006, he was a Monitor with the Department of Mathematics, IST, where he is currently an Invited Assistant Professor with the Department of Electrical and Computer Engineering. His research interests include sensor-based navigation and control of autonomous vehicles. Dr. Batista has received the Diploma de Mérito twice during his graduation and his Ph.D. thesis was awarded the Best Robotics Ph.D. Thesis Award by the Portuguese Society of Robotics.

Carlos Silvestre (M'07) received the Licenciatura degree in Electrical Engineering from the Instituto Superior Técnico (IST) of Lisbon, Portugal, in 1987 and the M.Sc. degree in Electrical Engineering and the Ph.D. degree in Control Science from the same school in 1991 and 2000, respectively. In 2011 he received the Habilitation in Electrical Engineering and Computers also from IST. Since 2000, he is with the Department of Electrical Engineering of the Instituto Superior Técnico, where he is currently an Associate Professor of Control and Robotics on leave. Since 2015 he is a Professor of the Department of Electrical and Computers Engineering of the Faculty of Science and Technology of the University of Macau. Over the past years, he has conducted research on the subjects of navigation guidance and control of air and underwater robots. His research interests include linear and nonlinear control theory, coordinated control of multiple vehicles, gain scheduled control, integrated design of guidance and control systems, inertial navigation systems, and mission control and real time architectures for complex autonomous systems with applications to unmanned air and underwater vehicles.

Paulo Oliveira (SM'10) received the Ph.D. degree in 2002 from the Instituto Superior Técnico (IST), Lisbon, Port-ugal. He is currently an Associate Professor with the Department of Mechanical Engineering, IST, Lisbon, Portugal, Researcher in the IDMEC/LAETA and collaborator in the ISR/LARSyS, Lisbon, Portugal. His research interests include Mechatronics, Robotics, and Estimation with special focus on the fields of sensor fusion, navigation, and control. He has participated in more than 20 Portuguese and European Research projects over the last 25 years.